Arabian Journal of Chemistry (2022) **15**, 103608

King Saud University

Arabian Journal of Chemistry

www.ksu.edu.sa
www.sciencedirect.com

ORIGINAL ARTICLE

Multiple machine learning models for prediction of CO_2 solubility in potassium and sodium based amino acid salt solutions

Guanwei Yin [a,*], Fouad Jameel Ibrahim Alazzawi [b], Dmitry Bokov [c,d], Haydar Abdulameer Marhoon [e,f], A.S. El-Shafay [g,h], Md Lutfor Rahman [i,*], Chia-Hung Su [j,*], Yi-Ze Lu [j], Hoang Chinh Nguyen [k]

[a] *School of Chemistry and Chemical Engineering, Inner Mongolia University, Inner Mongolia Autonomous Region, Hohhot 010000, China*
[b] *Computer Engineering Department, Al-Rafidain University College, Baghdad, Iraq*
[c] *Institute of Pharmacy, Sechenov First Moscow State Medical University, 8 Trubetskaya St., bldg. 2, Moscow 119991, Russian Federation*
[d] *Laboratory of Food Chemistry, Federal Research Center of Nutrition, Biotechnology and Food Safety, 2/14 Ustyinsky pr., Moscow 109240, Russian Federation*
[e] *Information and Communication Technology Research Group, Scientific Research Center, Al-Ayen University, Thi-Qar, Iraq*
[f] *College of Computer Sciences and Information Technology, University of Kerbala, Karbala, Iraq*
[g] *Department of Mechanical Engineering, College of Engineering, Prince Sattam bin Abdulaziz University, Alkharj 11942, Saudi Arabia*
[h] *Department of Mechanical Power Engineering, Faculty of Engineering, Mansoura University, Egypt*
[i] *Faculty of Science and Natural Resources, Universiti Malaysia Sabah, 88400 Kota Kinabalu, Sabah, Malaysia*
[j] *Department of Chemical Engineering, Ming Chi University of Technology, New Taipei City, Taiwan*
[k] *Faculty of Applied Sciences, Ton Duc Thang University, Ho Chi Minh City 700000, Viet Nam*

Received 15 August 2021; accepted 2 December 2021
Available online 9 December 2021

KEYWORDS

CO_2 solubility;
Artificial intelligence;

Abstract In this work, we developed artificial intelligence-based models for prediction and correlation of CO_2 solubility in amino acid solutions for the purpose of CO_2 capture. The models were used to correlate the process parameters to the CO_2 loading in the solvent. Indeed, CO_2 loading/-

* Corresponding authors.
E-mail addresses: lotfor@ums.edu.my (M. Lutfor Rahman), chsu@mail.mcut.edu.tw (C.-H. Su).

Peer review under responsibility of King Saud University.

Production and hosting by Elsevier

https://doi.org/10.1016/j.arabjc.2021.103608

Multi-layer Perceptron;
Decision tree;
AdaBoost

solubility in the solvent was considered as the sole model's output. The studied solvent in this work were potassium and sodium-based amino acid salt solutions. For the predictions, we tried three potential models, including Multi-layer Perceptron (MLP), Decision Tree (DT), and AdaBoost-DT. In order to discover the ideal hyperparameters for each model, we ran the method multiple times to find out the best model. R^2 scores for all three models exceeded 0.9 after optimization confirming the great prediction capabilities for all models. AdaBoost-DT indicated the highest R^2 Score of 0.998. With an R^2 of 0.98, Decision Tree was the second most accurate one, followed by MLP with an R^2 of 0.9.

1. Introduction

Development of models for prediction of CO_2 solubility in various solvents is a subject of great interest in order to develop efficient process for CO_2 capture (Nakhjiri and Heydarinasab, 2020; Pishnamazi, 2020; Nakhjiri, 2018; Nakhjiri, 2018; Marjani, 2020; Cao, 2021; Nakhjiri, 2018; Nakhjiri, 2020). From environmental point of view, it is crucial to implement proper engineered methodology as protective action for environment (Li, 2021; Shinde et al., 2021; Naddaf et al., 2021; Xu, 2021; Tjahjono, 2021; Ngafwan, 2021; Al-Shawi, 2021). Although various processes can be utilized for CO_2 capture from gas streams, absorption using chemical solvents is the attractive method for industrial applications due to its versatility and maturity of the process. Indeed, absorption is a gas–liquid operation which is driven based on mass transfer between gas and liquid phases with wide applications such as environment (Razzaq, 2021; Qaderi, 2020; Davoodnia, 2009). The mass transfer driving force can be enhanced by using a solvent which has great affinity towards the target component which is CO_2 (Wu, 2020; Wang, 2022; Won Lee, 2021; Geng, 2021). Indeed, mass transfer rate and consequently the separation efficiency can be enhanced by selection of a solvent by which the CO_2 solubility is high. However, examination and screening the appropriate solvents for a process is time consuming and costly, therefore predictive models can be employed for this purpose (Zajmi et al., 2018; Alsunki, 2020).

Predictive models have been already used in design and optimization of CO_2 capture processes such as membrane-based absorption systems in which the mass transfer and fluid dynamics of the process is simulated using mechanics or non-mechanistic models (Marjani, 2020; Rezakazemi et al., 2019; Dashti, 2018; Fadaei, 2012; Asadollahzadeh, 2018; Sohrabi, 2011; Dashti, 2020; Marjani, 2021; Razavi et al., 2015; Razavi et al., 2016; Shirazian et al., 2012; Razavi, 2016; Shirazian, 2017). Usually, mechanistic models based on computational fluid dynamics are used for simulation of CO_2 capture processes, however artificial intelligence-based models can be utilized in order to predict the solubility of CO_2 in a wide range of solvents. These artificial intelligence-based models rely on measured process data for fitting and training the model. Indeed, the data are used for training the network, and then validation is performed to assess the capability of the model in simulating the process data. Recently, combined and hybrid artificial intelligence-based algorithms have been developed and implemented to simulate chemical processing unit operations (Rezakazemi et al., 2019; Dashti, 2018; Ismail, 2019; Rezakazemi, 2018; Babanezhad, 2019; Cao, 2020; Nabipour, 2020; Soroush, 2019).

For prediction of CO_2 loading in chemical solvents, a number of machine learning methods have been implemented in which the model is used for screening the solvent and correlating the CO_2 solubility to process parameters. Soroush et al. (Alkawaz et al., 2020) predicted the solubility of CO_2 in various amino acid salt solutions via ANFIS method which is an artificial intelligence technique. The model indicated promising results with great accuracy in prediction of CO_2 loading as a function of input variables. Indeed, artificial intelligence models can be employed in this area to predict the solubility of CO_2 in different chemical and physical solvents. The results can be useful to choose the best solvent for a particular application. So, the cost and time of solvent selection and testing can be minimized by development of a robust predictive model for CO_2 loading. Machine learning (ML) techniques need measured data for simulation of processes and have attracted attention in wide areas of science and engineering (Dashti, 2018; Ismail, 2019; Rezakazemi, 2018; Wu, 2020; Deng et al., 2021; Wu, 2020; Farajnezhad, 2016; Rezakazemi et al., 2013; Khansary et al., 2017; Marjani et al., 2011; Rosenblatt, 1958).

In this work, we developed a comprehensive computational strategy for prediction of CO_2 solubility in various amino acid solutions. Three distinct artificial intelligence-based models are selected and implemented to the collected data of CO_2 solubility. We collected medium-sized numerical data on CO_2 solubility in potassium- and sodium-based amino acid salt solutions in this study. With six inputs: T (K), weight percent (wt.%), P_{CO2} (kPa), M_W-am, MP_C, MW_C, and alpha (solubility/loading) as the only output, we have a complete system of data for simulation (Alkawaz et al., 2020). Because of this fact, we must choose the appropriate models for predicting that are accurate and proportional to these differences in size. As a result, MLP (Multi-layer Perceptron), k-nearest Neighbors, extreme random trees, AdaBoost, Bagging Regressors, and some other models can be used to achieve this goal for these datasets. This is because data with a reduced dimensionality may be more prone to overfitting. We also need to be as precise as possible when defining the Hyper-parameters for each machine learning model. As a result, testing the data in various setups is a crucial stage in this investigation, and the results are interpreted and discussed to find out the best model for prediction of the dataset.

2. Modeling

In this study, a dataset consisting of the loading of CO_2 in solutions of amino acid salts versus input parameters were used for the modeling. The data are collected from literature and used in the artificial intelligence modeling (Alkawaz et al., 2020). Six inputs were considered in the model including temperature (T), solution concentration (wt%), CO_2 partial pressure (P_{CO2}), amino acid salt molecular weight (M_W-am), melting point of amino acid salt (MP_C), and molecular weight of cation (MW_C), while the CO_2 loading (alfa) was considered as the sole predicted output. Three different modeling approaches were employed which are defined in the following sections.

2.1. Multi-layer Perceptron (MLP) model

Frank Rosenblatt in (Agirre-Basurko et al., 2006) invented the Multi-Layer Perceptron (MLP), which is made up of several perceptrons or neurons. MLPs are generally arranged in three layers as it is shown in Fig. 1, known as the input layer, the hidden layer (which can contain more than one stack of neurons), and the output layer. Indeed, this type of configuration is known as an Artificial Neural Network (ANN). N neurons are located in the input layer, S neurons are in the hidden layer, and L neurons are located in the output layer as shown in Fig. 1.

Each input of the neurons x_i is associated with a weight w_i and calculated through Equation (1):

$$z = x_1 w_1 + \cdots + x_n w_n = X^T W \tag{1}$$

The activation function is then computed as f(z), where f(z) can be any continuously differentiable function such as a linear function, sigmoid function, or even the newer ReLU frequently employed in deep learning. After the perceptron evaluates the inputs and activates the relevant activation functions, the results are transferred to a classifier, which generates a probability distribution and "guesses" the proper label for the data. After collecting results using backpropagation methods, the weights are then changed for future inputs.

2.2. Decision tree (DT) model

The second model that was employed in this study is Decision Tree (DT). Because of the expansion of data mining methods, decision trees are becoming increasingly prominent in data analytics. It's basically an algorithm for classification and regression of data according to a set of criteria. In order to fit the data, the conventional method is recursive partitioning, a top-down, greedy algorithm (Quinlan, 1986). Some of the most common Decision Tree algorithms are ID3 (Quinlan, 1993), C4.5 (Quinlan, 1993; Timofeev, 2004), CART (van Diepen and Franses, 2006), and the chi-squared automatic interaction detector tree (CHAID) (Perner et al., 2001). The decision tree has a significant advantage over other modeling techniques in that it generates a model that can represent interpretable rules or logic statements. An important feature is the ability to explain trees that produce axis parallel decision surfaces (Yang, 2017).

For example, in Fig. 2 we can see an example of decision tree for Energy Efficiency Heating. In this figure boxes indicate terminal leaf nodes with labels within, whereas circles represent other nodes with a symbol inside referring to the feature where the split occurs. On the corresponding pathways, the dividing rules are provided.

2.3. AdaBoost-DT model

AdaBoost (Adaptive Boosting) (Makni and Zine, 2016) is an ensemble method that boosts weak estimators (DT in this study) to make a strong and more accurate regressor. It begins by fitting a regressor on the original dataset, and then fits further copies of the regressor on the same dataset, but with weights of instances changed based to the error of current prediction. Regressors that come after them focus more on tough situations as a result of this [63]. Algorithm of this methods is shown in Fig. 3.

2.4. Accuracy criteria of models

Like any regression modeling project, we need to split whole data into test and train data. A quarter of all data is utilized for testing and not for training a model, hence test data is a quarter of all data. For the simulation of solubility data, the remaining three-fourth of the data are used in the training phase. For the sake of comparison and determining the best model and the accuracy of the final job, we employed several criteria. Both test and train data were used to determine the coefficient of determination (R^2). Equation (2) calculates R^2, or the coefficient of determination:

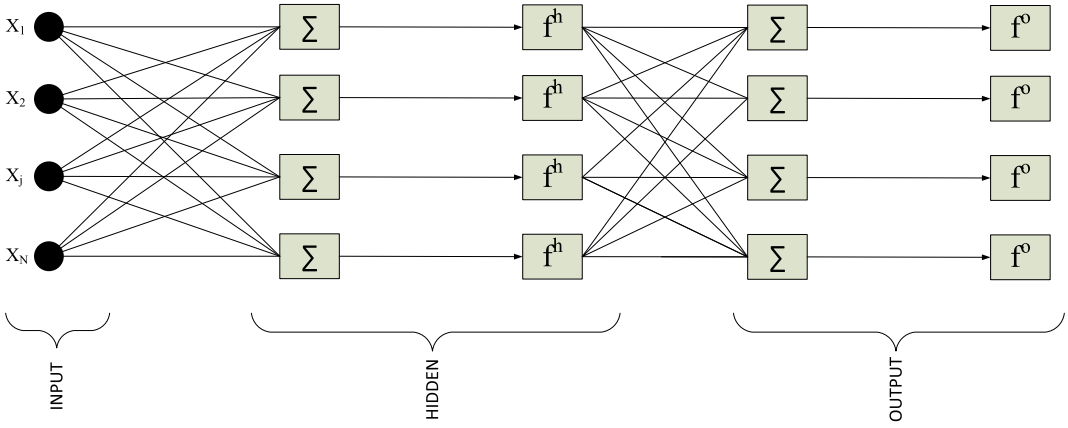

Fig. 1 A multilayer perceptron-based model (Ture, 2005).

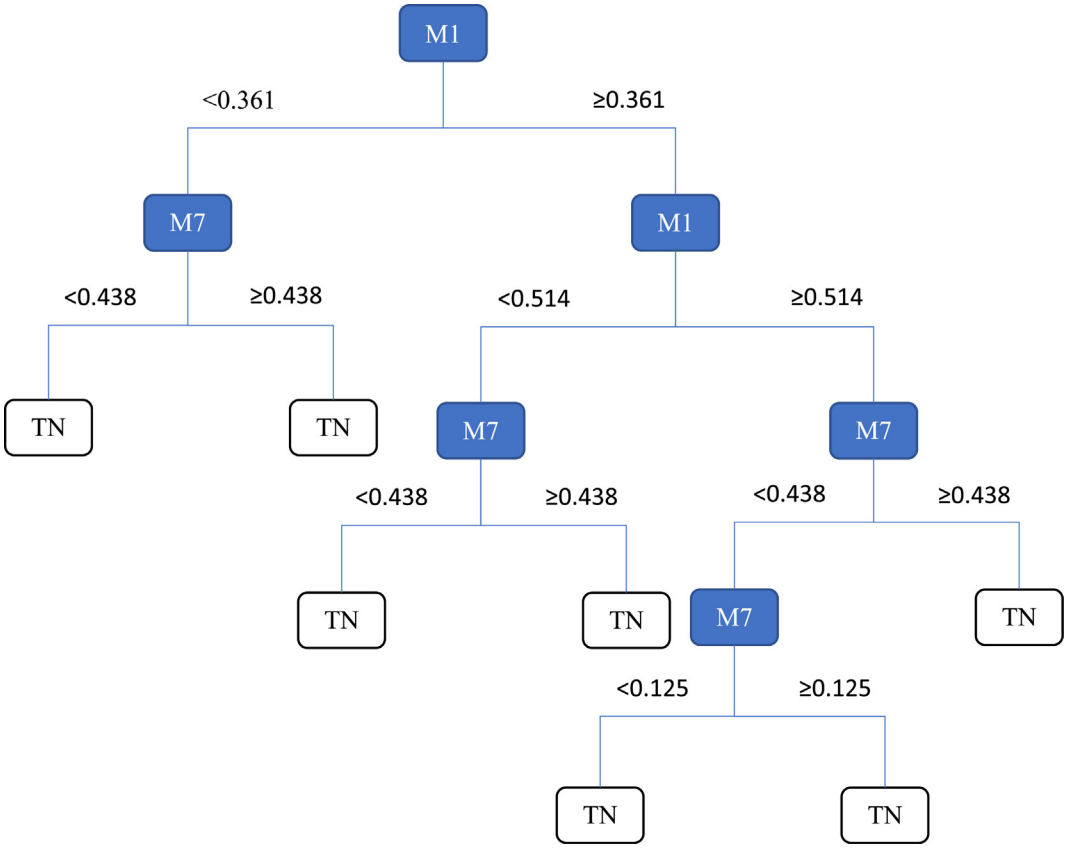

Fig. 2 Example of DT for Energy Efficiency Heating (Freund and Schapire, 1997).

a. Initialize D_1 (t) = 1/m
b. For number of iteration t = 1..., T
c. Train base learner using distribution Dt
d. Get base classifier h_t : X →ℜ
e. Choose a_t ∈ℜ
f. Update

$$D_{t+1}(i) = \frac{D_t(i)\exp(-ay_i h_t(x_i))}{Z_t}$$

g. Output of final classifier is given by:

$$H(x) = sign(\sum_{t=1}^{T} a_t h_t(x))$$

Fig. 3 AdaBoost Algorithm.

$$R^2 = 1 - \frac{u}{v} \quad (2)$$

where:

$$u = \sum_i (Q_i - y_i)^2 \quad (3)$$

$$v = \sum_i (\bar{y} - y_i)^2 \quad (4)$$

The k-fold cross-validation is the other requirement to implement the modeling of CO_2 solubility data. We employed the k-fold method to ensure that we don't run into the problem of overfitting. When it came time to find out how complex the model should be trained, we utilized three-fold cross-validation with k = 3. Finally, we also used MSE, RMSE and MAE metrics to compare the results of simulations generated by the models.

3. Results and discussions

3.1. Model selection

Besides comparing the models, we need to adjust certain other crucial hyper-parameters to gain better accuracy. A variety of configurations were used to test the data in order to optimize other parameters. To simulate using MLP, we need to tweak the hidden layer sizes, maximum iterations, and alpha values, among other things. As a result, we experimented with numerous values for these factors in order to find the optimum one. Table 1 lists some of the most accurate configurations employed in this study.

Table 2 Selected Parameters for MLP.

Parameter	Value
Hidden layer size	100
Max Iteration	1500
Alpha	0.001

Changes of error rate on increasing hidden layer sizes are shown in Fig. 4. We can adjust this parameter near to 100 using this chart. Now we need tunning for alpha. A number of various values of this parameter have also been tried in the model based on available experimental data. These results

Table 1 Accuracy of different configs of MLP.

Max Depth	Hidden layer size	alpha	Train R^2	Test R^2	RMSE	MSE	Mean absolute error
1500	95	0.001	0.91088	0.89817	2.06E-01	4.23E-02	1.20E-01
1000	95	0.001	0.91088	0.89817	2.06E-01	4.23E-02	1.20E-01
2500	95	0.001	0.91088	0.89817	2.06E-01	4.23E-02	1.20E-01
2000	95	0.001	0.91088	0.89817	2.06E-01	4.23E-02	1.20E-01
3000	95	0.001	0.91088	0.89817	2.06E-01	4.23E-02	1.20E-01
1000	65	0.01	0.9078	0.89308	2.13E-01	4.56E-02	1.27E-01
3000	65	0.01	0.9078	0.89308	2.13E-01	4.56E-02	1.27E-01
2500	65	0.01	0.9078	0.89308	2.13E-01	4.56E-02	1.27E-01
1500	65	0.01	0.9078	0.89308	2.13E-01	4.56E-02	1.27E-01
2000	65	0.01	0.9078	0.89308	2.13E-01	4.56E-02	1.27E-01
1000	95	0.0001	0.89877	0.88487	2.12E-01	4.48E-02	1.20E-01
3000	95	0.0001	0.89877	0.88487	2.12E-01	4.48E-02	1.20E-01
1500	95	0.0001	0.89877	0.88487	2.12E-01	4.48E-02	1.20E-01
2000	95	0.0001	0.89877	0.88487	2.12E-01	4.48E-02	1.20E-01
2500	95	0.0001	0.89877	0.88487	2.12E-01	4.48E-02	1.20E-01
3000	95	0.01	0.88533	0.86868	2.24E-01	5.00E-02	1.24E-01

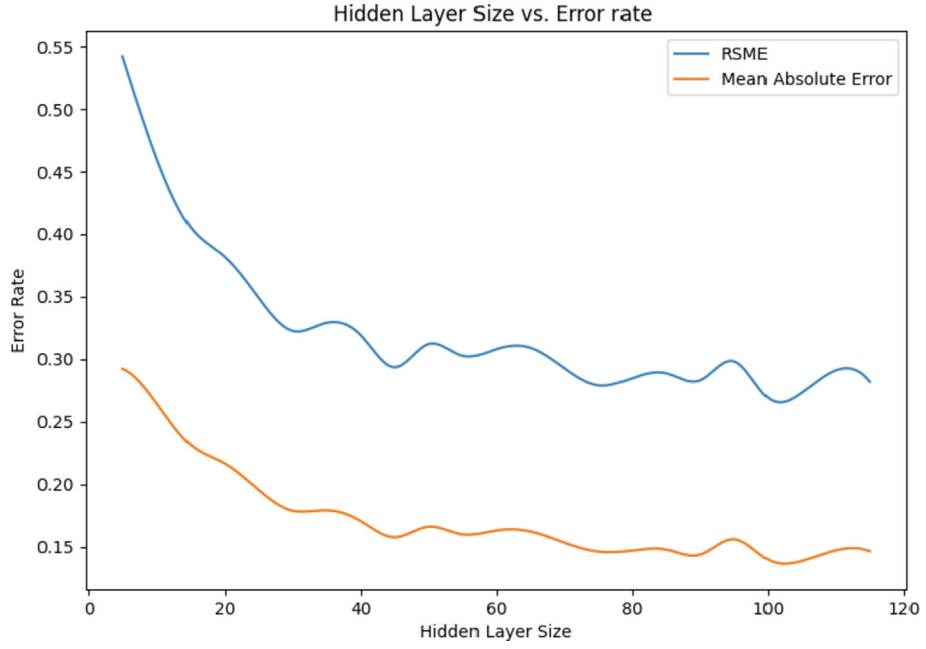

Fig. 4 Error rate with Hidden Layer Size changes.

Table 3 Top Accurate Configurations for Decision Tree.

Criterion	Max Tree Depth	Train R^2	Test R^2	RMSE	MSE	Mean absolute error
Mae	9	0.98785	0.92622	2.09E-01	4.36E-02	1.45E-01
Mae	8	0.9759	0.9167	2.20E-01	4.83E-02	1.52E-01
Mse	9	0.99006	0.9089	2.09E-01	4.35E-02	1.38E-01
friedman_mse	9	0.99006	0.90693	2.11E-01	4.46E-02	1.39E-01
Mse	7	0.96771	0.90436	2.17E-01	4.69E-02	1.55E-01
friedman_mse	7	0.96771	0.90436	2.17E-01	4.69E-02	1.55E-01
friedman_mse	8	0.98237	0.90327	2.14E-01	4.60E-02	1.45E-01
Mse	8	0.98237	0.90321	2.15E-01	4.61E-02	1.45E-01
Mae	7	0.95507	0.89379	2.45E-01	6.02E-02	1.72E-01
Mse	6	0.94386	0.88197	2.38E-01	5.66E-02	1.71E-01

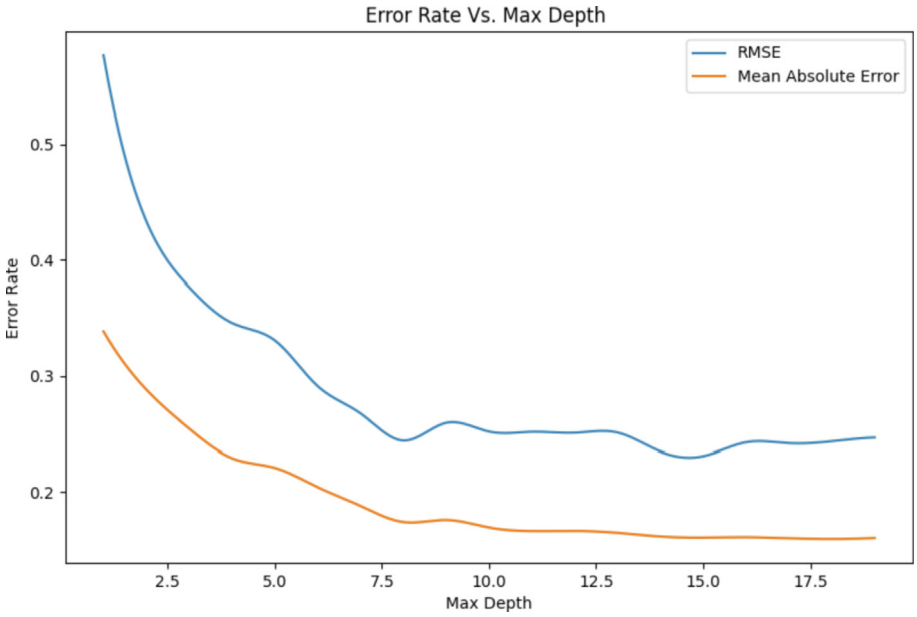

Fig. 5 Effect of maximum depth change on error rate in the decision tree model.

Table 4 Top Accurate Configurations for AdaBoost-DT.

Number of DTs	Max Depth	Train R^2	Test R^2	RMSE	MSE	Mean absolute error
40	9	0.99759	0.93888	1.70E-01	2.89E-02	1.07E-01
50	9	0.99765	0.93888	1.70E-01	2.90E-02	1.07E-01
60	9	0.99766	0.93846	1.71E-01	2.92E-02	1.08E-01
55	9	0.99765	0.93812	1.72E-01	2.94E-02	1.08E-01
45	9	0.99756	0.93757	1.72E-01	2.96E-02	1.08E-01
30	9	0.99729	0.93748	1.72E-01	2.95E-02	1.07E-01
35	9	0.99743	0.93695	1.72E-01	2.97E-02	1.08E-01
25	9	0.99727	0.9359	1.73E-01	3.00E-02	1.07E-01
20	9	0.99707	0.93587	1.74E-01	3.01E-02	1.06E-01
15	9	0.99671	0.93217	1.76E-01	3.11E-02	1.10E-01
70	8	0.99462	0.92923	1.82E-01	3.30E-02	1.15E-01
60	8	0.99436	0.92833	1.83E-01	3.34E-02	1.15E-01
80	9	0.99772	0.92363	1.88E-01	3.52E-02	1.09E-01
65	9	0.99771	0.92359	1.87E-01	3.51E-02	1.10E-01
130	9	0.99781	0.92347	1.88E-01	3.53E-02	1.08E-01
70	9	0.99767	0.92343	1.87E-01	3.51E-02	1.09E-01
85	9	0.99774	0.92324	1.88E-01	3.54E-02	1.09E-01
95	9	0.99782	0.92307	1.88E-01	3.55E-02	1.08E-01

suggest a value of 0.001 for alpha. After these tests, we will use the primary factors presented in Table 2 to create a final MLP model.

For DT Model we need to do tunning for two important hyper-parameters: (1) maximum tree depth and criterion that is the function to measure the quality of a split. To do this, more than 300 different combinations were tested, some of the highest accuracy recorded in Table 3.

In Fig. 5 we show how error rate of DT changes on increasing maximum tree depth. According to these table and figure, following combination have chosen for final DT model: Criterion = mae, max_depth = 9.

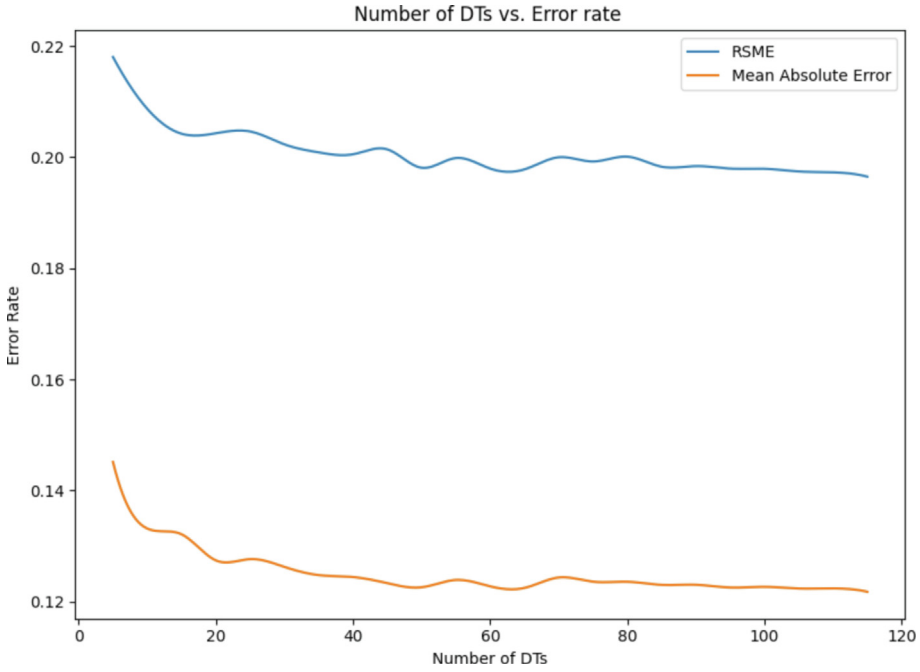

Fig. 6 Effect of Number of Estimators change on error rate in AdaBoost-DT.

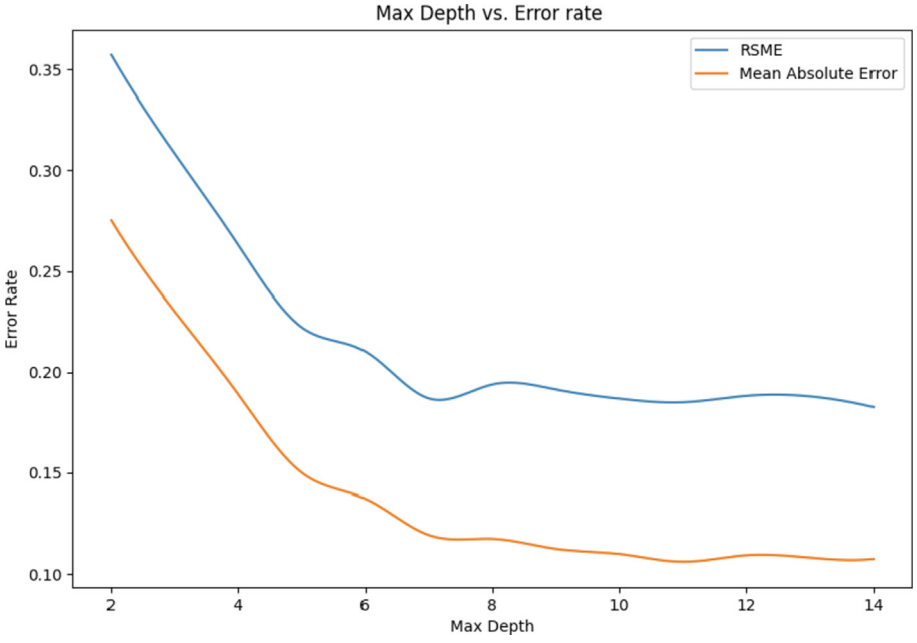

Fig. 7 Effect of Max Tree Depth change on error rate in AdaBoost-DT.

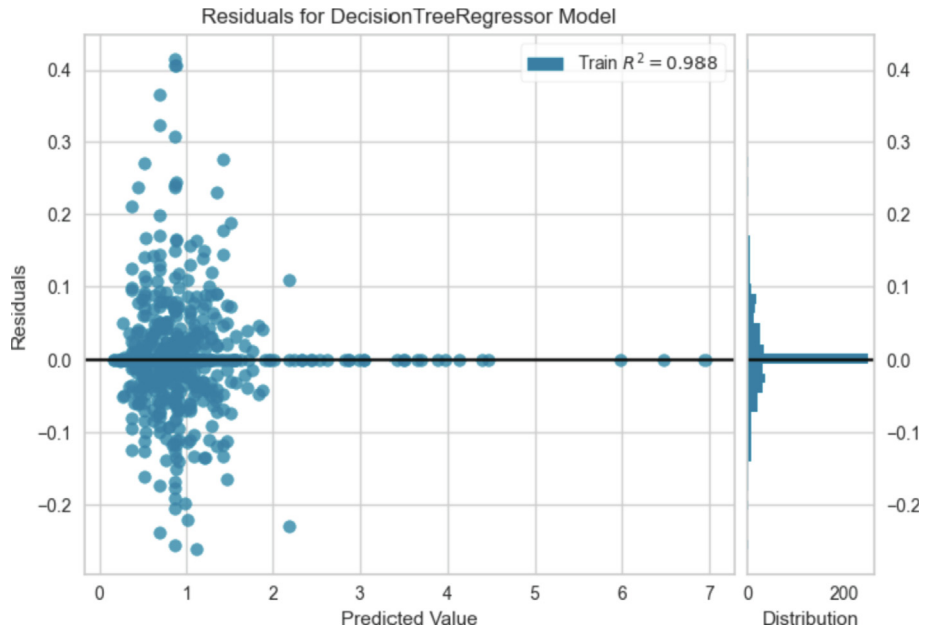

Fig. 8 Residuals on selected DT model.

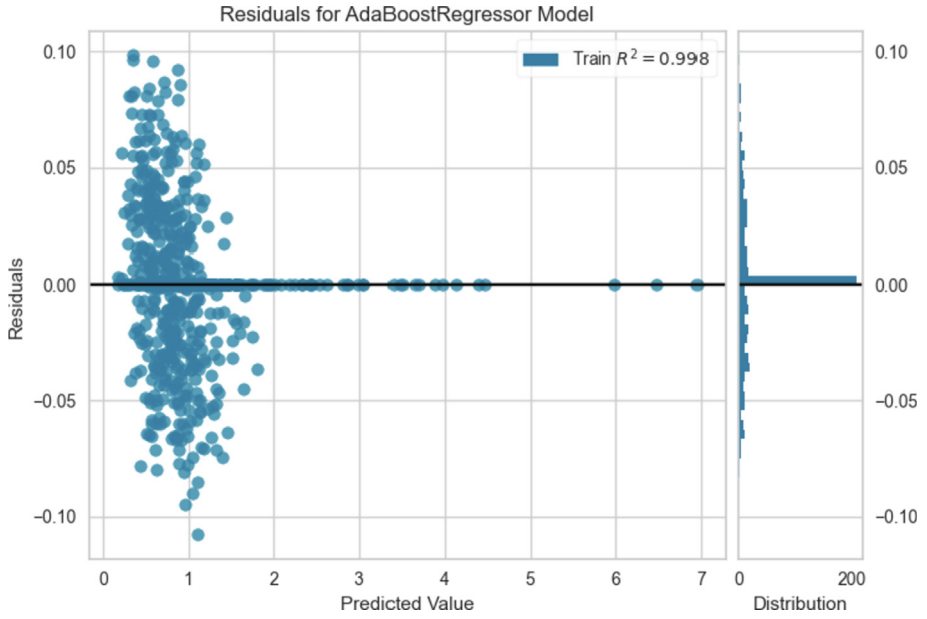

Fig. 9 Residuals on selected AdaBoost-DT model.

Table 5 Final Models results.

Model	MSE	RMSE	Mean absolute error	Train R^2
MLP	5.5179E-02	2.3490E-05	2. 03467E-01	0.894
Decision Tree	4.9836E-02	2.2324E-01	1.47467E-01	0.988
AdaBoost-DT	3.6094E-02	1.8998E-01	1.10790E-01	0.998

As the last step, Hyper-parameter selection for number of estimators employed in the third model, AdaBoost with DT as a weak learner, must also be improved along with maximum depth. It's all laid out in Table 4 and Fig. 6. The random AdaBoost-DT also uses the criteria mse, N estimators = 50, and Max Depth = 9 (see Fig. 7).

3.2. Model analysis

In this section, we test our data using the models specified in the previous section. Determining the importance of features is one of the comparative advantages of AdaBoost-DT, and some other tree-based models. So, after finding the best config-

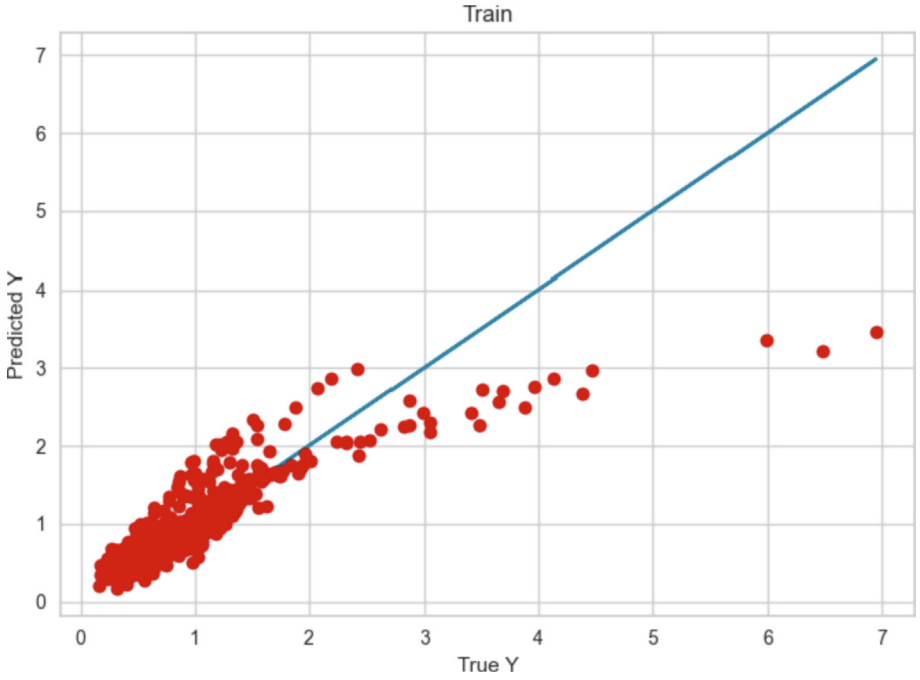

Fig. 10 Comparing Train prediction with true output (MLP Model).

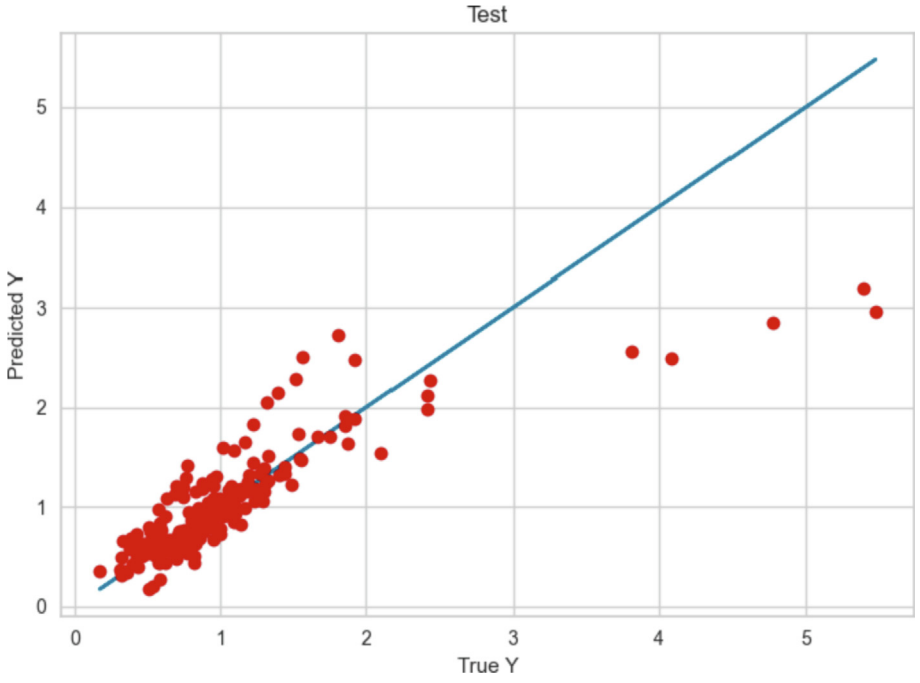

Fig. 11 Comparing Test prediction with true output (MLP Model).

uration of our AdaBoost-DT model, we can show importance of fractures on Fig. 8, and also on Fig. 9 we can see this importance. Furthermore, the final model results in terms of comparison are listed in Table 5. It is clearly observed that AdaBoost-DT indicated the best performance for fitting the solubility data.

A comparison between Figs. 8 and 9 shows the relative agreement of these values with two different models. Also,

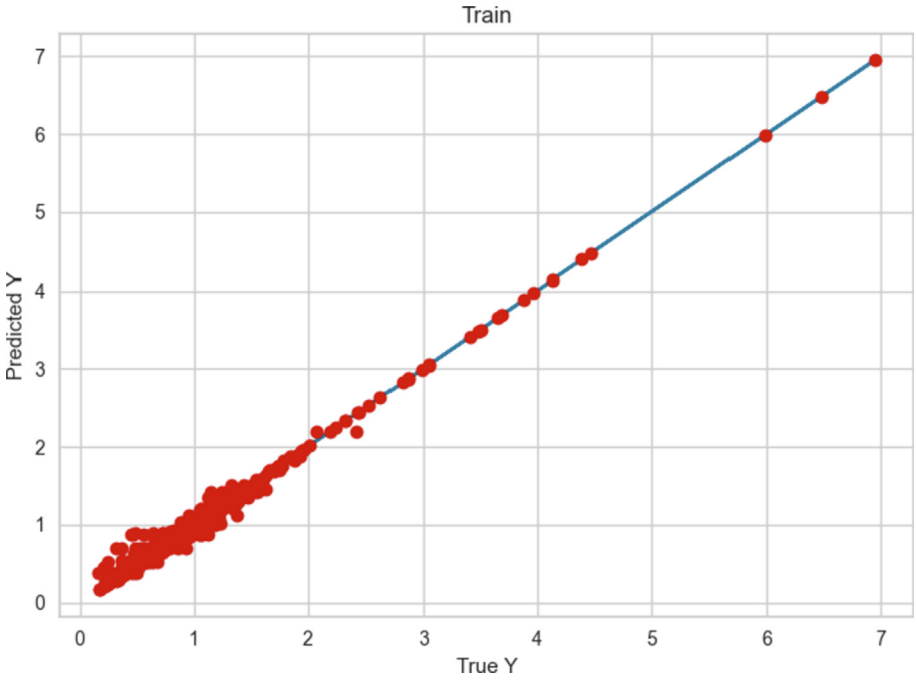

Fig. 12 Comparing Train prediction with true output (DT Model).

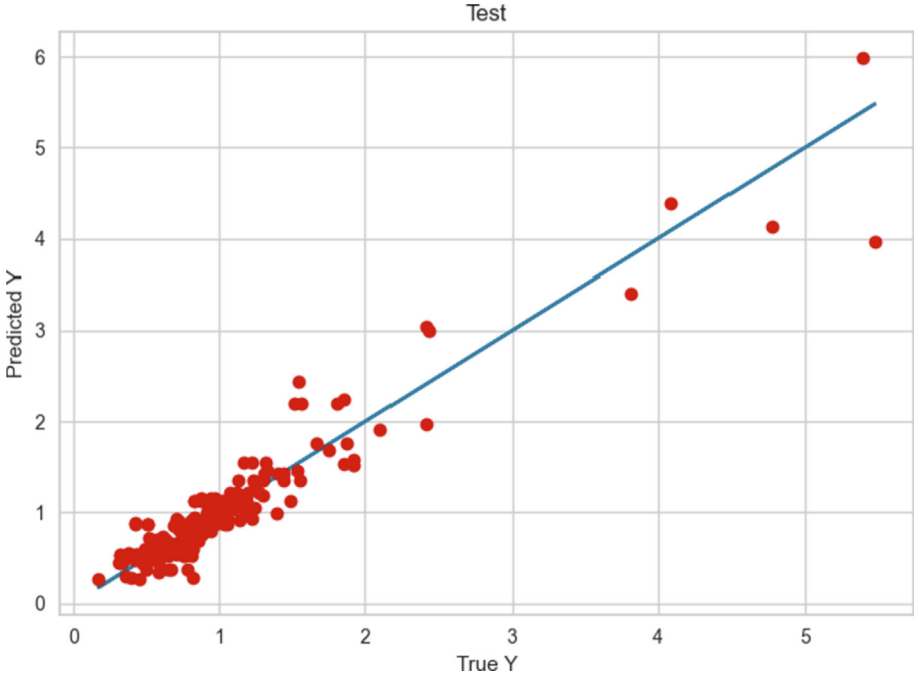

Fig. 13 Comparing Test prediction with true output (DT Model).

Figs. 10-15 indicate the comparisons of predicted and actual values for the training and testing stages for all three models used in this work. From Figs. 10 to 15, it is clear that the AdaBoost-DT is more closely aligned with the expected outcome than either of the other two models.

The trained and tested models were then used to evaluate the importance of each parameter on the CO_2 loading, and the results for AdaBoost-DT and DT are represented in Figs. 16 and 17, respectively. It is seen that in AdaBoost-DT model, the weight percentage of solvent has the most impor-

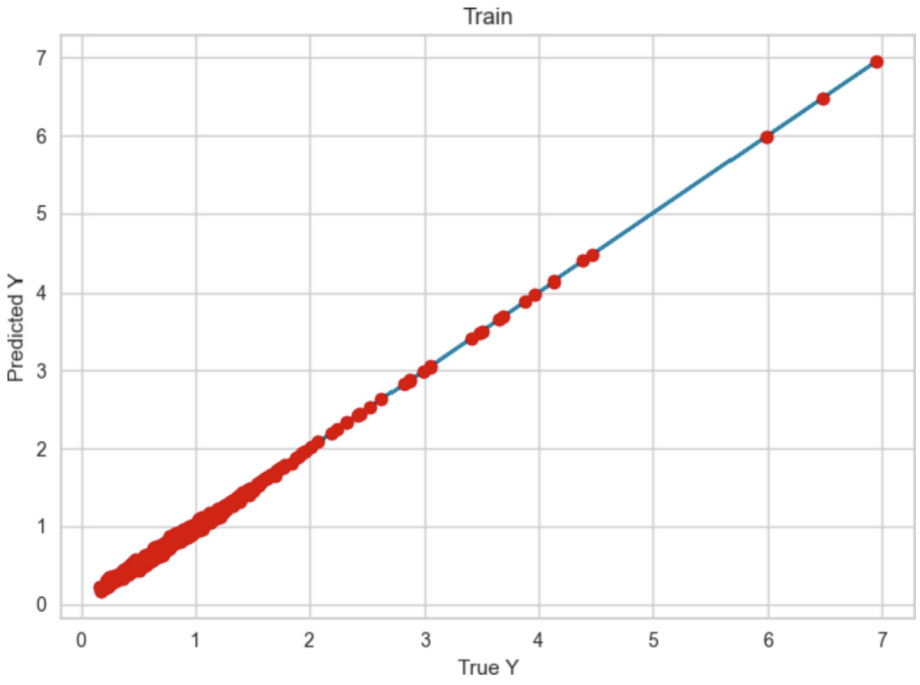

Fig. 14 Comparing Train prediction with true output (AdaBoost-DT Model).

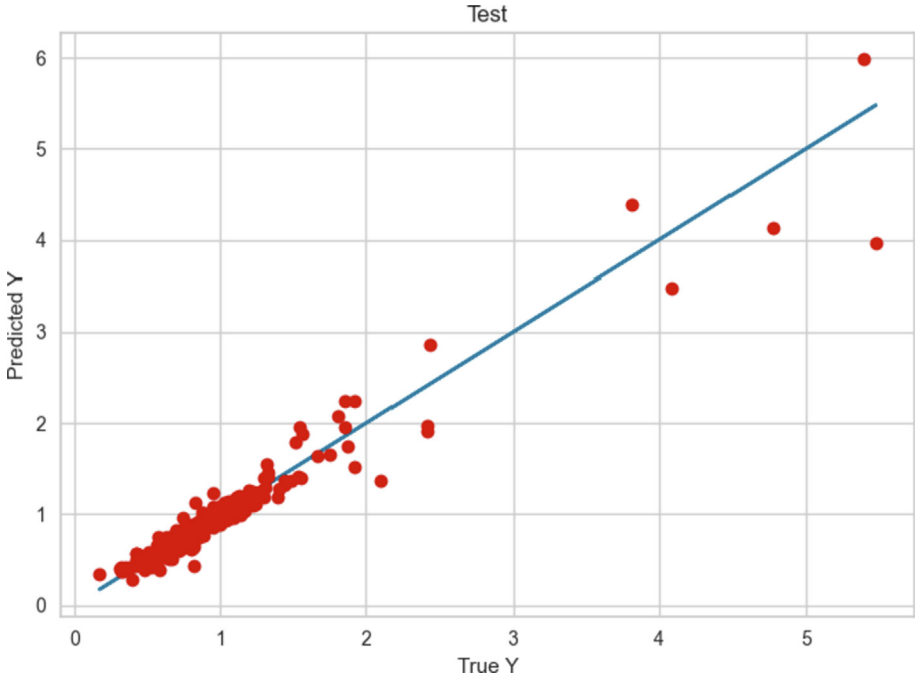

Fig. 15 Comparing Test prediction with true output (AdaBoot-DT Model).

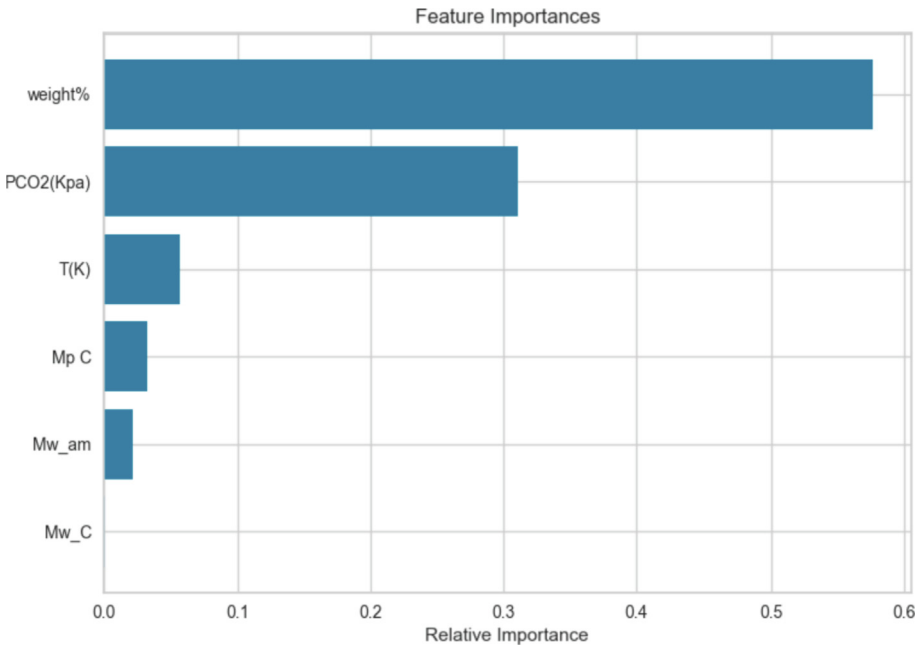

Fig. 16 Feature Importance using AdaBoost-DT.

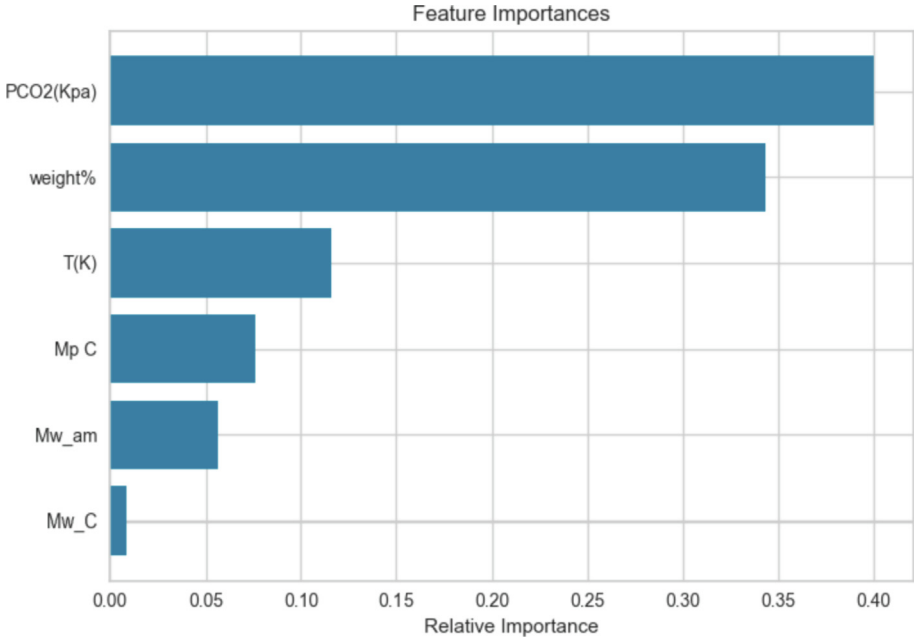

Fig. 17 Feature Importance using DT.

tant influence on the CO_2 loading, while the cation molecular weight shows the least importance effect. For both models, it is seen that CO_2 partial pressure and weight percentage are the most important parameters. Finally, the effect of P_{CO2} (kPa) and weight% on the solubility of CO_2 shown in Fig. 18 depicts the AdaBoost model. Both P_{CO2} (kPa) and weight percent have a considerable impact on CO_2 solubility.

4. Conclusion

We carried out a comprehensive simulation based on artificial intelligence to predict the solubility of CO_2 in amino acid salt solutions. In the simulation of CO_2 solubility, we created and analyzed a variety of supervised learning algorithms. The literature-sourced data on CO_2 solubility was incorporated

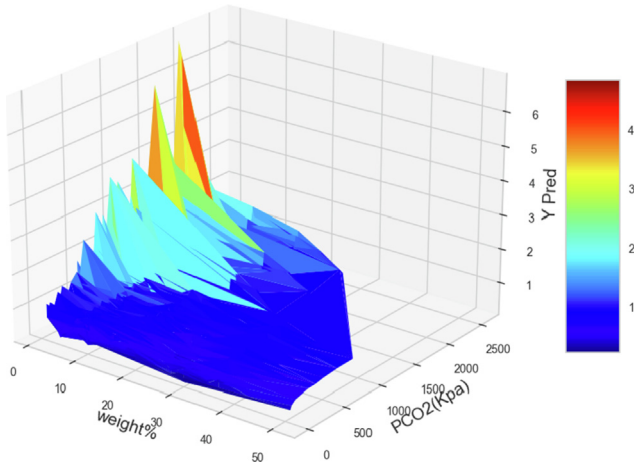

Fig. 18 The effect of P_{CO2}(kPa) and weight% on CO_2 solubility predicted by the AdaBoost-DT model.

into the simulations for training and validation. Instead of only employing these models, the Hyper-parameters were tuned to improve the anticipated results. The Mean absolute error criterion reduced the error to 1.10790E-01, and the R^2 score rose to 0.998 as a result. The results indicated that AdaBoost-DT showed the best performance in predicting CO_2 loading.

Declaration of Competing Interest

The authors declare that they have no known competing financial interests or personal relationships that could have appeared to influence the work reported in this paper.

Reference

Nakhjiri, A.T., Heydarinasab, A., 2020. CFD Analysis of CO2 Sequestration Applying Different Absorbents Inside the Microporous PVDF Hollow Fiber Membrane Contactor. Periodica Polytechnica Chemical Engineering 64 (1), 135–145.

Pishnamazi, M. et al, 2020. Computational investigation on the effect of [Bmim][BF4] ionic liquid addition to MEA alkanolamine absorbent for enhancing CO2 mass transfer inside membranes 113635.

Nakhjiri, A.T. et al, 2018. The effect of membrane pores wettability on CO2 removal from CO2/CH4 gaseous mixture using NaOH, MEA and TEA liquid absorbents in hollow fiber membrane contactor. Chinese Journal of Chemical Engineering 26 (9), 1845–1861.

Nakhjiri, A.T. et al, 2018. Experimental investigation and mathematical modeling of CO2 sequestration from CO2/CH4 gaseous mixture using MEA and TEA aqueous absorbents through polypropylene hollow fiber membrane contactor. Journal of Membrane Science 565, 1–13.

Marjani, A. et al, 2020. Mass transfer modeling CO2 absorption using nanofluids in porous polymeric membranes. Journal of Molecular Liquids 114115.

Cao, Y. et al, 2021. Mathematical modeling and numerical simulation of CO2 capture using MDEA-based nanofluids in nanostructure membranes. Process Safety and Environmental Protection.

Nakhjiri, A.T. et al, 2018. Modeling and simulation of CO2 separation from CO2/CH4 gaseous mixture using potassium glycinate, potassium argininate and sodium hydroxide liquid absorbents in the hollow fiber membrane contactor. Journal of Environmental Chemical Engineering 6 (1), 1500–1511.

Nakhjiri, A.T. et al, 2020. *Numerical simulation of CO_2/H_2S simultaneous removal from natural gas using potassium carbonate aqueous solution in hollow fiber membrane contactor*. Journal of Environmental. Chemical Engineering 104130.

Li, A. et al, 2021. Developing the non-dimensional framework for water distribution formulation to evaluate sprinkler irrigation*. Irrigation and Drainage 70 (4), 659–667.

shinde, R.S., N.S. Korde, and R.A. More, *Green synthesis, characterization and biological activity of aryl Azo Schiff bases*. Journal of Applied Organometallic Chemistry, 2021. **1**(4): p. 165-173.

Naddaf, M.E., Lotfi, M., Tohidfar, M., 2021. In vitro Regeneration of Persian Melon (Cucumis melo) CV. Khatooni through Direct Organogenesis. Journal of Plant Bioinformatics and Biotechnology 1 (2), 97–102.

Xu, Y.-P. et al, 2021. Optimal structure design of a PV/FC HRES using amended Water Strider Algorithm. Energy Reports 7, 2057–2067.

Tjahjono, T. et al, 2021. Role of Cryogenic Cycling Rejuvenation on Flow Behavior of ZrCuAlNiAg Metallic Glass at Relaxation Temperature. Transactions of the Indian Institute of Metals 74 (12), 3241–3247.

Ngafwan, N. et al, 2021. Study on novel fluorescent carbon nanomaterials in food analysis. Ciência e Tecnologia de Alimentos, 1–6.

Al-Shawi, S.G. et al, 2021. Synthesis of NiO Nanoparticles and Sulfur, and Nitrogen co Doped-Graphene Quantum Dots/ NiO Nanocomposites for Antibacterial Application. Journal of Nanostructures 11 (1), 181–188.

Razzaq, A. et al, 2021. Asymmetric inter-linkages between green technology innovation and consumption-based carbon emissions in BRICS countries using quantile-on-quantile framework. Technology in Society 66, 101656.

Qaderi, J., 2020. A brief review on the reaction mechanisms of CO_2 hydrogenation into methanol. International Journal of Innovative Research and Scientific Studies 3 (2), 33–40.

Davoodnia, A. et al, 2009. Bronsted-acidic ionic liquid [HO3S(CH2) 4MIM][HSO4] as efficient and reusable catalyst for one-pot synthesis of beta-acetamido ketones. Monatshefte für Chemie - Chemical Monthly 140, 1499–1502.

Wu, J. et al, 2020. Analysis on full CO2 capture schemes in NG/O2 combustion gas and steam mixture cycle (GSMC). Energy 191, 116470.

Wang, C. et al, 2022. Electrowinning-coupled CO2 capture with energy-efficient absorbent regeneration: Towards practical application. Chemical Engineering Journal 427, 131981.

Won Lee, J. et al, 2021. *Liquid-like adsorbent assembled by CNTs: serving as renewable CO2 capture materials for indoor air*. Journal of Energy. Chemistry.

Geng, Y.-Q. et al, 2021. Research progress of calcium-based adsorbents for CO2 capture and anti-sintering modification. Journal of Fuel Chemistry and Technology 49 (7), 998–1013.

Zajmi, L., Ahmed, F.Y.H., Jaharadak, A.A., 2018. Concepts, Methods, and Performances of Particle Swarm Optimization, Backpropagation, and Neural Networks. Applied Computational Intelligence and Soft Computing 2018, 9547212.

Alsunki, A.A.M. et al, 2020. Framework of Software Developers Engagement Antecedents and Productivity - A Review. in *2020 16th IEEE International Colloquium on Signal Processing & Its Applications (CSPA)*.

Rezakazemi, M., Mosavi, A., Shirazian, S., 2019. ANFIS pattern for molecular membranes separation optimization. Journal of Molecular Liquids 274, 470–476.

Dashti, A. et al, 2018. Estimating CH4 and CO2 solubilities in ionic liquids using computational intelligence approaches. Journal of Molecular Liquids 271, 661–669.

Fadaei, F. et al, 2012. Mass transfer simulation of ion separation by nanofiltration considering electrical and dielectrical effects. Desalination 284, 316–323.
Asadollahzadeh, M. et al, 2018. Simulation of Nonporous Polymeric Membranes Using CFD for Bioethanol Purification. Macromolecular Theory and Simulations 27 (3).
Sohrabi, M.R. et al, 2011. Theoretical Studies on Membrane-Based Gas Separation using Computational Fluid Dynamics (CFD) of Mass Transfer. Journal of the Chemical Society of Pakistan 33 (4), 464–473.
Dashti, A. et al, 2020. Computational Simulation of CO_2 Sorption in Polymeric Membranes Using Genetic Programming. Arabian Journal for Science and Engineering.
Marjani, A. et al, 2021. Evaluation of potassium glycinate, potassium lysinate, potassium sarcosinate and potassium threonate solutions in CO2 capture using membranes. Arabian Journal of Chemistry 14, (3) 102979.
Razavi, S.M.R., Shirazian, S., Najafabadi, M.S., 2015. Investigations on the Ability of Di-Isopropanol Amine Solution for Removal of CO2 From Natural Gas in Porous Polymeric Membranes. Polymer Engineering and Science 55 (3), 598–603.
Razavi, S.M.R., Shirazian, S., Nazemian, M., 2016. Numerical simulation of CO2 separation from gas mixtures in membrane modules: Effect of chemical absorbent. Arabian Journal of Chemistry 9 (1), 62–71.
Shirazian, S., Marjani, A., Rezakazemi, M., 2012. Separation of CO2 by single and mixed aqueous amine solvents in membrane contactors: fluid flow and mass transfer modeling. Engineering with Computers 28 (2), 189–198.
Razavi, S.M.R. et al, 2016. Simulation of CO2 absorption by solution of ammonium ionic liquid in hollow-fiber contactors. Chemical Engineering and Processing: Process Intensification 108, 27–34.
Shirazian, S. et al, 2017. Artificial neural network modelling of continuous wet granulation using a twin-screw extruder. International Journal of Pharmaceutics 521 (1–2), 102–109.
Ismail, H.Y. et al, 2019. Developing ANN-Kriging hybrid model based on process parameters for prediction of mean residence time distribution in twin-screw wet granulation. Powder Technology 343, 568–577.
Rezakazemi, M. et al, 2018. Development of hybrid models for prediction of gas permeation through FS/POSS/PDMS nanocomposite membranes. International Journal of Hydrogen Energy 43 (36), 17283–17294.
Babanezhad, M. et al, 2019. Liquid-phase chemical reactors: Development of 3D hybrid model based on CFD-adaptive network-based fuzzy inference system. Canadian Journal of Chemical Engineering 97, 1676–1684.
Cao, Y. et al, 2020. Prediction of fluid pattern in a shear flow on intelligent neural nodes using ANFIS and LBM. Neural Computing & Applications 32 (17), 13313–13321.
Nabipour, N. et al, 2020. Prediction of Nanofluid Temperature Inside the Cavity by Integration of Grid Partition Clustering Categorization of a Learning Structure with the Fuzzy System. Acs Omega 5 (7), 3571–3578.
Soroush, E. et al, 2019. ANFIS modeling for prediction of CO_2 solubility in potassium and sodium based amino acid Salt solutions. Journal of Environmental Chemical Engineering 7, (1) 102925.
Alkawaz, M.H., Veeran, M.T., Bachok, R., 2020. Digital Image Forgery Detection based on Expectation Maximization Algorithm. in *2020 16th IEEE International Colloquium on Signal Processing & Its Applications (CSPA)*.
Wu, H. et al, 2020. A geometric accuracy analysis and tolerance robust design approach for a vertical machining center based on the reliability theory. Measurement 161, 107809.
Deng, Z., Liu, C., Zhu, Z., 2021. Inter-hours rolling scheduling of behind-the-meter storage operating systems using electricity price forecasting based on deep convolutional neural network. International Journal of Electrical Power & Energy Systems 125, 106499.
Wu, H. et al, 2020. Robust design method for optimizing the static accuracy of a vertical machining center. The International Journal of Advanced Manufacturing Technology 109 (7), 2009–2022.
Farajnezhad, A. et al, 2016. Correlation of interaction parameters in Wilson, NRTL and UNIQUAC models using theoretical methods. Fluid Phase Equilibria 417, 181–186.
Rezakazemi, M., Marjani, A., Shirazian, S., 2013. Development of a Group Contribution Method Based on UNIFAC Groups for the Estimation of Vapor Pressures of Pure Hydrocarbon Compounds. Chemical Engineering & Technology 36 (3), 483–491.
Khansary, M.A., Marjani, A., Shirazian, S., 2017. On the search of rigorous thermo-kinetic model for wet phase inversion technique. Journal of Membrane Science 538, 18–33.
Marjani, A., Rezakazemi, M., Shirazian, S., 2011. Vapor pressure prediction using group contribution method. Oriental Journal of Chemistry 27 (4), 1331–1335.
Rosenblatt, F., 1958. The perceptron: A probabilistic model for information storage and organization in the brain. Psychological Review 65 (6), 386–408.
Agirre-Basurko, E., Ibarra-Berastegi, G., Madariaga, I., 2006. Regression and multilayer perceptron-based models to forecast hourly O3 and NO2 levels in the Bilbao area. Environmental Modelling & Software 21 (4), 430–446.
Ture, M. et al, 2005. Comparing classification techniques for predicting essential hypertension. Expert Systems with Applications 29 (3), 583–588.
Quinlan, J.R., *Induction of decision trees*. Machine Learning, 1986. **1** (1): p. 81-106.
Quinlan, J.R., *CHAPTER 4 - Pruning Decision Trees*, in *C4.5*, J.R. Quinlan, Editor. 1993, Morgan Kaufmann: San Francisco (CA). p. 35-43.
Quinlan, J.R., *CHAPTER 5 - From Trees to Rules*, in *C4.5*, J.R. Quinlan, Editor. 1993, Morgan Kaufmann: San Francisco (CA). p. 45-56.
Timofeev, R. *Classification and Regression Trees(CART)Theory and Applications*. 2004.
van Diepen, M., Franses, P.H., 2006. Evaluating chi-squared automatic interaction detection. Information Systems 31 (8), 814–831.
Perner, P., Zscherpel, U., Jacobsen, C., 2001. A comparison between neural networks and decision trees based on data from industrial radiographic testing. Pattern Recognition Letters 22 (1), 47–54.
Yang, L. et al, 2017. A regression tree approach using mathematical programming. Expert Systems with Applications 78, 347–357.
Freund, Y., Schapire, R.E., 1997. A Decision-Theoretic Generalization of On-Line Learning and an Application to Boosting. Journal of Computer and System Sciences 55 (1), 119–139.
Makni, Z., Zine, W., 2016. Rotor position estimator based on machine learning. in IECON 2016–42nd Annual Conference of the IEEE Industrial Electronics Society.